22. DARK MATTER

Revised September 2011 by M. Drees (Bonn University) and G. Gerbier (Saclay, CEA).

22.1. Theory

22.1.1. *Evidence for Dark Matter* :

The existence of Dark (*i.e.*, non-luminous and non-absorbing) Matter (DM) is by now well established [1,2]. The earliest, and perhaps still most convincing, evidence for DM came from the observation that various luminous objects (stars, gas clouds, globular clusters, or entire galaxies) move faster than one would expect if they only felt the gravitational attraction of other visible objects. An important example is the measurement of galactic rotation curves. The rotational velocity v of an object on a stable Keplerian orbit with radius r around a galaxy scales like $v(r) \propto \sqrt{M(r)/r}$, where $M(r)$ is the mass inside the orbit. If r lies outside the visible part of the galaxy and mass tracks light, one would expect $v(r) \propto 1/\sqrt{r}$. Instead, in most galaxies one finds that v becomes approximately constant out to the largest values of r where the rotation curve can be measured; in our own galaxy, $v \simeq 240$ km/s at the location of our solar system, with little change out to the largest observable radius. This implies the existence of a *dark halo*, with mass density $\rho(r) \propto 1/r^2$, *i.e.*, $M(r) \propto r$; at some point ρ will have to fall off faster (in order to keep the total mass of the galaxy finite), but we do not know at what radius this will happen. This leads to a lower bound on the DM mass density, $\Omega_{\rm DM} \gtrsim 0.1$, where $\Omega_X \equiv \rho_X/\rho_{\rm crit}$, $\rho_{\rm crit}$ being the critical mass density (*i.e.*, $\Omega_{\rm tot} = 1$ corresponds to a flat Universe).

The observation of clusters of galaxies tends to give somewhat larger values, $\Omega_{\rm DM} \simeq 0.2$. These observations include measurements of the peculiar velocities of galaxies in the cluster, which are a measure of their potential energy if the cluster is virialized; measurements of the *X-ray* temperature of hot gas in the cluster, which again correlates with the gravitational potential felt by the gas; and—most directly—studies of (weak) gravitational lensing of background galaxies on the cluster.

A particularly compelling example involves the bullet cluster (1E0657-558) which recently (on cosmological time scales) passed through another cluster. As a result, the hot gas forming most of the clusters' baryonic mass was shocked and decelerated, whereas the galaxies in the clusters proceeded on ballistic trajectories. Gravitational lensing shows that most of the total mass also moved ballistically, indicating that DM self-interactions are indeed weak [1].

The currently most accurate, if somewhat indirect, determination of $\Omega_{\rm DM}$ comes from global fits of cosmological parameters to a variety of observations; see the Section on Cosmological Parameters for details. For example, using measurements of the anisotropy of the cosmic microwave background (CMB) and of the spatial distribution of galaxies, Ref. 3 finds a density of cold, non-baryonic matter

$$\Omega_{\rm nbm} h^2 = 0.112 \pm 0.006 \ , \tag{22.1}$$

where h is the Hubble constant in units of 100 km/(s·Mpc). Some part of the baryonic matter density [3],

$$\Omega_{\rm b} h^2 = 0.022 \pm 0.001 \ , \tag{22.2}$$

may well contribute to (baryonic) DM, *e.g.*, MACHOs [4] or cold molecular gas clouds [5].

The DM density in the "neighborhood" of our solar system is also of considerable interest. This was first estimated as early as 1922 by J.H. Jeans, who analyzed the motion of nearby stars transverse to the galactic plane [2]. He concluded that in our galactic neighborhood, the average density of DM must be roughly equal to that of luminous matter (stars, gas, dust). Remarkably enough, the most recent estimate, based on a detailed model of our galaxy constrained by a host of observables including the galactic rotation curve, finds a quite similar result for the smooth component of the local Dark Matter density [6]:

$$\rho_{\rm DM}^{\rm local} = (0.39 \pm 0.03) \frac{\rm GeV}{\rm cm^3} \ . \tag{22.3}$$

This value may have to be increased by a factor of 1.2 ± 0.2 since the baryons in the galactic disk, in which the solar system is located, also increase the local DM density [7]. Small substructures (minihaloes, streams) are not likely to change the local DM density significantly [1].

22.1.2. *Candidates for Dark Matter* :

Analyses of structure formation in the Universe indicate that most DM should be "cold" or "cool", *i.e.*, should have been non-relativistic at the onset of galaxy formation (when there was a galactic mass inside the causal horizon) [1]. This agrees well with the upper bound [3] on the contribution of light neutrinos to Eq. (22.1),

$$\Omega_\nu h^2 \leq 0.0062 \quad 95\% \text{ CL} \ . \tag{22.4}$$

Candidates for non-baryonic DM in Eq. (22.1) must satisfy several conditions: they must be stable on cosmological time scales (otherwise they would have decayed by now), they must interact very weakly with electromagnetic radiation (otherwise they wouldn't qualify as *dark* matter), and they must have the right relic density. Candidates include primordial black holes, axions, sterile neutrinos, and weakly interacting massive particles (WIMPs).

Primordial black holes must have formed before the era of Big-Bang nucleosynthesis, since otherwise they would have been counted in Eq. (22.2) rather than Eq. (22.1). Such an early creation of a large number of black holes is possible only in certain somewhat contrived cosmological models [8].

The existence of axions [9] was first postulated to solve the strong *CP* problem of QCD; they also occur naturally in superstring theories. They are pseudo Nambu-Goldstone bosons associated with the (mostly) spontaneous breaking of a new global "Peccei-Quinn" (PQ) U(1) symmetry at scale f_a; see the Section on Axions in this *Review* for further details. Although very light, axions would constitute cold DM, since they were produced non-thermally. At temperatures well above the QCD phase transition, the axion is massless, and the axion field can take any value, parameterized by the "misalignment angle" θ_i. At $T \lesssim 1$ GeV, the axion develops a mass m_a due to instanton effects. Unless the axion field happens to find itself at the minimum of its potential ($\theta_i = 0$), it will begin to oscillate once m_a becomes comparable to the Hubble parameter H. These coherent

oscillations transform the energy originally stored in the axion field into physical axion quanta. The contribution of this mechanism to the present axion relic density is [1]

$$\Omega_a h^2 = \kappa_a \left(f_a / 10^{12}\ \mathrm{GeV} \right)^{1.175} \theta_i^2 \ , \tag{22.5}$$

where the numerical factor κ_a lies roughly between 0.5 and a few. If $\theta_i \sim \mathcal{O}(1)$, Eq. (22.5) will saturate Eq. (22.1) for $f_a \sim 10^{11}$ GeV, comfortably above laboratory and astrophysical constraints [9]; this would correspond to an axion mass around 0.1 meV. However, if the post-inflationary reheat temperature $T_R > f_a$, cosmic strings will form during the PQ phase transition at $T \simeq f_a$. Their decay will give an additional contribution to Ω_a, which is often bigger than that in Eq. (22.5) [1], leading to a smaller preferred value of f_a, *i.e.*, larger m_a. On the other hand, values of f_a near the Planck scale become possible if θ_i is for some reason very small.

"Sterile" $SU(2) \times U(1)_Y$ singlet neutrinos with keV masses [10] could alleviate the "cusp/core problem" [1] of cold DM models. If they were produced non-thermally through mixing with standard neutrinos, they would eventually decay into a standard neutrino and a photon.

Weakly interacting massive particles (WIMPs) χ are particles with mass roughly between 10 GeV and a few TeV, and with cross sections of approximately weak strength. Within standard cosmology, their present relic density can be calculated reliably if the WIMPs were in thermal and chemical equilibrium with the hot "soup" of Standard Model (SM) particles after inflation. In this case, their density would become exponentially (Boltzmann) suppressed at $T < m_\chi$. The WIMPs therefore drop out of thermal equilibrium ("freeze out") once the rate of reactions that change SM particles into WIMPs or vice versa, which is proportional to the product of the WIMP number density and the WIMP pair annihilation cross section into SM particles σ_A times velocity, becomes smaller than the Hubble expansion rate of the Universe. After freeze out, the co-moving WIMP density remains essentially constant; if the Universe evolved adiabatically after WIMP decoupling, this implies a constant WIMP number to entropy density ratio. Their present relic density is then approximately given by (ignoring logarithmic corrections) [11]

$$\Omega_\chi h^2 \simeq const. \cdot \frac{T_0^3}{M_{\rm Pl}^3 \langle \sigma_A v \rangle} \simeq \frac{0.1\ \mathrm{pb} \cdot c}{\langle \sigma_A v \rangle} \ . \tag{22.6}$$

Here T_0 is the current CMB temperature, $M_{\rm Pl}$ is the Planck mass, c is the speed of light, σ_A is the total annihilation cross section of a pair of WIMPs into SM particles, v is the relative velocity between the two WIMPs in their cms system, and $\langle \ldots \rangle$ denotes thermal averaging. Freeze out happens at temperature $T_F \simeq m_\chi/20$ almost independently of the properties of the WIMP. This means that WIMPs are already non-relativistic when they decouple from the thermal plasma; it also implies that Eq. (22.6) is applicable if $T_R > T_F$. Notice that the 0.1 pb in Eq. (22.6) contains factors of T_0 and $M_{\rm Pl}$; it is, therefore, quite intriguing that it "happens" to come out near the typical size of weak interaction cross sections.

The seemingly most obvious WIMP candidate is a heavy neutrino. However, an SU(2) doublet neutrino will have too small a relic density if its mass exceeds $M_Z/2$, as required by LEP data. One can suppress the annihilation cross section, and hence increase the relic density, by postulating mixing between a heavy SU(2) doublet and some sterile neutrino. However, one also has to require the neutrino to be stable; it is not obvious why a massive neutrino should not be allowed to decay.

The currently best motivated WIMP candidate is, therefore, the lightest superparticle (LSP) in supersymmetric models [12] with exact R-parity (which guarantees the stability of the LSP). Searches for exotic isotopes [13] imply that a stable LSP has to be neutral. This leaves basically two candidates among the superpartners of ordinary particles, a sneutrino, and a neutralino. The negative outcome of various WIMP searches (see below) rules out "ordinary" sneutrinos as primary component of the DM halo of our galaxy. (In models with gauge-mediated SUSY breaking, the lightest "messenger sneutrino" could make a good WIMP [14].) The most widely studied WIMP is therefore the lightest neutralino. Detailed calculations [1] show that the lightest neutralino will have the desired thermal relic density Eq. (22.1) in at least four distinct regions of parameter space. χ could be (mostly) a bino or photino (the superpartner of the $U(1)_Y$ gauge boson and photon, respectively), if both χ and some sleptons have mass below ~ 150 GeV, or if m_χ is close to the mass of some sfermion (so that its relic density is reduced through co-annihilation with this sfermion), or if $2m_\chi$ is close to the mass of the *CP*-odd Higgs boson present in supersymmetric models. Finally, Eq. (22.1) can also be satisfied if χ has a large higgsino or wino component.

Many non-supersymmetric extensions of the Standard Model also contain viable WIMP candidates [1]. Examples are the lightest $T-$odd particle in "Little Higgs" models with conserved $T-$parity, or "techni-baryons" in scenarios with an additional, strongly interacting ("technicolor" or similar) gauge group.

There also exist models where the DM particles, while interacting only weakly with ordinary matter, have quite strong interactions within an extended "dark sector" of the theory. These were motivated by measurements by the PAMELA, ATIC and Fermi satellites indicating excesses in the cosmic e^+ and/or e^- fluxes at high energies. However, these excesses are relative to background estimates that are clearly too simplistic (*e.g.*, neglecting primary sources of electrons and positrons, and modeling the galaxy as a homogeneous cylinder). Moreover, the excesses, if real, are far too large to be due to usual WIMPs, but can be explained by astrophysical sources. It therefore seems unlikely that they are due to Dark Matter [15]. Similarly, claims of positive signals for direct WIMP detection by the DAMA and, more recently, CoGeNT and CRESST collaborations (see below) led to the development of tailor-made models to alleviate tensions with null experiments. Since we are not convinced that these data indeed signal WIMP detection, and these models (some of which were quickly excluded by improved measurements) lack independent motivation, we will not discuss them any further in this Review.

Although thermally produced WIMPs are attractive DM candidates because their relic density naturally has at least the right order of magnitude, non-thermal production mechanisms have also been suggested, *e.g.*, LSP production from the decay of some moduli fields [16], from the decay of the inflaton [17], or from the decay of "$Q-$balls"

(non-topological solitons) formed in the wake of Affleck-Dine baryogenesis [18]. Although LSPs from these sources are typically highly relativistic when produced, they quickly achieve kinetic (but not chemical) equilibrium if T_R exceeds a few MeV [19](but stays below $m_\chi/20$). They therefore also contribute to cold DM. Finally, if the WIMPs aren't their own antiparticles, an asymmetry between WIMPs and antiWIMPs might have been created in the early Universe, possibly by the same (unknown) mechanism that created the baryon antibaryon asymmetry. In such "asymmetric DM" models [20] the WIMP antiWIMP annihilation cross section $\langle\sigma_A v\rangle$ should be significantly larger than $1\,\mathrm{pb}\cdot c$, cf Eq. (22.6).

Primary black holes (as MACHOs), axions, sterile neutrinos, and WIMPs are all (in principle) detectable with present or near-future technology (see below). There are also particle physics DM candidates which currently seem almost impossible to detect, unless they decay; the present lower limit on their lifetime is of order 10^{25} to 10^{26} s for 100 GeV particles. These include the gravitino (the spin-3/2 superpartner of the graviton) [1], states from the "hidden sector" thought responsible for supersymmetry breaking [14], and the axino (the spin-1/2 superpartner of the axion) [1].

22.2. Experimental detection of Dark Matter

22.2.1. *The case of baryonic matter in our galaxy* :

The search for hidden galactic baryonic matter in the form of MAssive Compact Halo Objects (MACHOs) has been initiated following the suggestion that they may represent a large part of the galactic DM and could be detected through the microlensing effect [4]. The MACHO, EROS, and OGLE collaborations have performed a program of observation of such objects by monitoring the luminosity of millions of stars in the Large and Small Magellanic Clouds for several years. EROS concluded that MACHOs cannot contribute more than 8% to the mass of the galactic halo [21], while MACHO observed a signal at 0.4 solar mass and put an upper limit of 40%. Overall, this strengthens the need for non-baryonic DM, also supported by the arguments developed above.

22.2.2. *Axion searches* :

Axions can be detected by looking for $a \to \gamma$ conversion in a strong magnetic field [1]. Such a conversion proceeds through the loop-induced $a\gamma\gamma$ coupling, whose strength $g_{a\gamma\gamma}$ is an important parameter of axion models. There currently are two experiments searching for axionic DM. They both employ high quality cavities. The cavity "Q factor" enhances the conversion rate on resonance, *i.e.*, for $m_a(c^2 + v_a^2/2) = \hbar\omega_{\mathrm{res}}$. One then needs to scan the resonance frequency in order to cover a significant range in m_a or, equivalently, f_a. The bigger of the two experiments, the ADMX experiment [22], originally situated at the LLNL in California but now running at the University of Washington, started taking data in the first half of 1996. It now uses SQUIDs as first-stage amplifiers; their extremely low noise temperature (1.2 K) enhances the conversion signal. Published results [23], combining data taken with conventional amplifiers and SQUIDs, exclude axions with mass between 1.9 and 3.53 μeV, corresponding to $f_a \simeq 4\cdot 10^{13}$ GeV, for an assumed local DM density of 0.45 GeV/cm^3, if $g_{a\gamma\gamma}$ is near the upper end of the

theoretically expected range. An about five times better limit on $g_{a\gamma\gamma}$ was achieved [24] for 1.98 μeV $\leq m_a \leq$ 2.18 μeV, if a large fraction of the local DM density is due to a single flow of axions with very low velocity dispersion. The ADMX experiment is being upgraded by reducing the cavity and SQUID temperature from the current 1.2 K to about 0.1 K. This should increase the frequency scanning speed for given sensitivity by more than two orders of magnitude, or increase the sensitivity for fixed observation time.

The smaller "CARRACK" experiment now being developed in Kyoto, Japan [25] uses Rydberg atoms (atoms excited to a very high state, $n = 111$) to detect the microwave photons that would result from axion conversion. This allows almost noise-free detection of single photons. Their ultimate goal is to probe the range between 2 and 50 μeV with sensitivity to all plausible axion models, if axions form most of DM.

22.2.3. *Searches for keV Neutrinos* :

Relic keV neutrinos ν_s can only be detected if they mix with the ordinary neutrinos. This mixing leads to radiative $\nu_s \to \nu\gamma$ decays, with lifetime $\tau_{\nu_s} \simeq 1.8 \cdot 10^{21}\ \mathrm{s} \cdot (\sin\theta)^{-2} \cdot (1\ \mathrm{keV}/m_{\nu_s})^5$, where θ is the mixing angle [10]. This gives rise to a flux of mono-energetic photons with $E_\gamma = m_{\nu_s}/2$, which might be observable by *X-ray* satellites. In the simplest case the relic ν_s are produced only by oscillations of standard neutrinos. Assuming that all lepton-antilepton asymmetries are well below 10^{-3}, the ν_s relic density can then be computed uniquely in terms of the mixing angle θ and the mass m_{ν_s}. The combination of lower bounds on m_{ν_s} from analyses of structure formation (in particular, the Lyα "forest") and upper bounds on *X-ray* fluxes from various (clusters of) galaxies exclude this scenario if ν_s forms all of DM. This conclusion can be evaded if ν_s forms only part of DM, and/or if there is a lepton asymmetry $\geq 10^{-3}$ (i.e. some 7 orders of magnitude above the observed baryon-antibaryon asymmetry), and/or if there is an additional source of ν_s production in the early Universe, e.g. from the decay of heavier particles [10].

22.2.4. *Basics of direct WIMP search* :

As stated above, WIMPs should be gravitationally trapped inside galaxies and should have the adequate density profile to account for the observed rotational curves. These two constraints determine the main features of experimental detection of WIMPs, which have been detailed in the reviews in [1].

Their mean velocity inside our galaxy relative to its center is expected to be similar to that of stars, *i.e.*, a few hundred kilometers per second at the location of our solar system. For these velocities, WIMPs interact with ordinary matter through elastic scattering on nuclei. With expected WIMP masses in the range 10 GeV to 10 TeV, typical nuclear recoil energies are of order of 1 to 100 keV.

The shape of the nuclear recoil spectrum results from a convolution of the WIMP velocity distribution, usually taken as a Maxwellian distribution in the galactic rest frame, shifted into the Earth rest frame, with the angular scattering distribution, which is isotropic to first approximation but forward-peaked for high nuclear mass (typically higher than Ge mass) due to the nuclear form factor. Overall, this results in a roughly exponential spectrum. The higher the WIMP mass, the higher the mean value of the exponential. This points to the need for low nuclear recoil energy threshold detectors.

On the other hand, expected interaction rates depend on the product of the local WIMP flux and the interaction cross section. The first term is fixed by the local density of dark matter, taken as 0.39 GeV/cm^3 [see Eq. (22.3)], the mean WIMP velocity, typically 220 km/s, the galactic escape velocity, typically 544 km/s [26] and the mass of the WIMP. The expected interaction rate then mainly depends on two unknowns, the mass and cross section of the WIMP (with some uncertainty [6] due to the halo model). This is why the experimental observable, which is basically the scattering rate as a function of energy, is usually expressed as a contour in the WIMP mass–cross section plane.

The cross section depends on the nature of the couplings. For non-relativistic WIMPs, one in general has to distinguish spin-independent and spin-dependent couplings. The former can involve scalar and vector WIMP and nucleon currents (vector currents are absent for Majorana WIMPs, *e.g.*, the neutralino), while the latter involve axial vector currents (and obviously only exist if χ carries spin). Due to coherence effects, the spin-independent cross section scales approximately as the square of the mass of the nucleus, so higher mass nuclei, from Ge to Xe, are preferred for this search. For spin-dependent coupling, the cross section depends on the nuclear spin factor; used target nuclei include ^{19}F, ^{23}Na, ^{73}Ge, ^{127}I, ^{129}Xe, ^{131}Xe, and ^{133}Cs.

Cross sections calculated in MSSM models [27] induce rates of at most 1 evt day^{-1} kg^{-1} of detector, much lower than the usual radioactive backgrounds. This indicates the need for underground laboratories to protect against cosmic ray induced backgrounds, and for the selection of extremely radio-pure materials.

The typical shape of exclusion contours can be anticipated from this discussion: at low WIMP mass, the sensitivity drops because of the detector energy threshold, whereas at high masses, the sensitivity also decreases because, for a fixed mass density, the WIMP flux decreases $\propto 1/m_\chi$. The sensitivity is best for WIMP masses near the mass of the recoiling nucleus.

Two important points are to be kept in mind when comparing exclusion curves from various experiments between them or with positive indications of a signal.

For an experiment with a fixed nuclear recoil energy threshold, the lower is the considered WIMP mass, the lower is the fraction of the spectrum to which the experiment is sensitive. This fraction may be extremely small in some cases. For instance CoGeNT [28], using a Germanium detector with an energy threshold of around 2 keV, is sensitive to about 10 % of the total recoil spectrum of a 7 GeV WIMP, while for XENON100 [29], using a liquid Xenon detector with a threshold of 8.4 keV, this fraction is only 0.05 % (that is the extreme tail of the distribution), for the same WIMP mass. The two experiments are then sensitive to very different parts of the WIMP velocity distribution.

A second important point to consider is the energy resolution of the detector. Again at low WIMP mass, the expected roughly exponential spectrum is very steep and when the characteristic energy of the exponential becomes of the same order as the energy resolution, the energy smearing becomes important. In particular, a significant fraction of the expected spectrum below effective threshold is smeared above threshold, increasing artificially the sensitivity. For instance, a Xenon detector with a threshold

of 8 keV and infinitely good resolution is actually insensitive to a 7 GeV mass WIMP, because the expected energy distribution has a cut-off at roughly 5 keV. When folding in the experimental resolution of XENON100 (corresponding to a photostatistics of 0.5 photoelectron per keV), then around 1 % of the signal is smeared above 5 keV and 0.05 % above 8 keV. Setting reliable cross section limits in this mass range thus requires a complete understanding of the response of the detector at energies well below the nominal threshold.

In order to homogenize the reliability of the presented exclusion curves, and save the reader the trouble of performing tedious (though easy to do) calculations, we propose to set cross section limits only for WIMP mass above a *"WIMP safe"* minimal mass value defined as the maximum of 1) the mass where the increase of sensitivity from infinite resolution to actual experimental resolution is not more than a factor two, and 2) the mass where the experiment is sensitive to at least 1 % of the total WIMP signal recoil spectrum. These recommendations are irrespective of the content of the experimental data obtained by the experiments.

22.2.5. *Status and prospects of direct WIMP searches* :

Given the intense activity of the field, readers interested in more details than the ones given below may refer to [1], as well as to presentations at recent conferences [30].

The first searches have been performed with ultra-pure semiconductors installed in pure lead and copper shields in underground environments. Combining a priori excellent energy resolutions and very pure detector material, they produced the first limits on WIMP searches (Heidelberg-Moscow, IGEX, COSME-II, HDMS) [1]. Planned experiments using several tens of kg to a ton of Germanium run at liquid nitrogen temperature (designed for double-beta decay search)—GERDA, MAJORANA—are based in addition on passive reduction of the external and internal electromagnetic and neutron background by using segmented detectors, minimal detector housing, close electronics, pulse shape discrimination and large liquid nitrogen or argon shields. Their sensitivity to WIMP interactions will depend on their ability to lower the energy threshold sufficiently, while keeping the background rate small.

The use of so called Point Contact Germanium detectors, with a very small capacitance allowing to reach sub-keV thresholds, has given rise to new results. The CoGeNT collaboration [31] has operated a single 440 g Germanium detector with an effective threshold of 400 eV in the Soudan Underground Laboratory for 56 days [28]. After applying a rise time cut on the pulse shapes in order to remove the surface interactions known to suffer from incomplete charge collection, the resulting spectrum below 4 keV is said by the authors to exhibit an irreducible excess of events, with energy spectrum roughly exponential, compatible with a light mass WIMP in the 7-11 GeV range, and cross section around 10^{-4} pb. However, this conclusion crucially depends on the energy dependent rise time cut applied to the data and a sizeable leaking of surface events into the kept spectrum cannot be excluded. The authors acknowledge themselves that a possible instrumental effect, leading to such an excess, is worth investigating. Nevertheless, considerable attention has been paid to the WIMP interpretation, largely due to the temptation to consider it as a confirmation of the low mass WIMP DAMA/LIBRA

solution, without channeling (see below). A recent unpublished analysis, presented at the TAUP 2011 conference, indicates a reduction of the claimed signal by a factor 10. Further results [32] based on data accumulated during one year led to the claim of a 2.8 sigma modulation said to be compatible with a WIMP. Here again, the claim is considerably weakened by the fact that the amplitude of the curve describing the expected WIMP modulation in the 0.5-3 keV bin is too high by roughly a factor 2 (or more, if the unmodulated "signal" has to be reduced) and wrongly leads to the conclusion that the modulation is compatible with a standard WIMP in a standard halo. This is also noted in [33].

A new consortium, CDEX/TEXONO, plans to build a 10 kg array of small and very low (200 eV) threshold detectors, and to operate them in the new Chinese Jinping underground laboratory, the deepest in the world.

In order to make further progress in the reliability of any claimed signal, active background rejection and signal identification questions have to be addressed. This is the focus of a growing number of investigations and improvements. Active background rejection in detectors relies on the relatively small ionization in nuclear recoils due to their low velocity. This induces a reduction ("quenching") of the ionization/scintillation signal for nuclear recoil signal events relative to e or γ induced backgrounds. Energies calibrated with gamma sources are then called "electron equivalent energies" (keVee unit used below). This effect has been both calculated and measured [1]. It is exploited in cryogenic detectors described later. In scintillation detectors, it induces in addition a difference in decay times of pulses induced by e/γ events vs nuclear recoils. In most cases, due to the limited resolution and discrimination power of this technique at low energies, this effect allows only a statistical background rejection. It has been used in NaI(Tl) (DAMA, LIBRA, NAIAD, Saclay NaI), in CsI(Tl) (KIMS), and Xe (ZEPLIN-I) [1,30]. Pulse shape discrimination is particularly efficient in liquid argon. Using a high energy threshold, it has been used for an event by event discrimination by the WARP experiment, but the high threshold also leads to a moderate signal sensitivity. No observation of nuclear recoils has been reported by these experiments.

Two experimental signatures are predicted for true WIMP signals. One is a strong daily forward/backward asymmetry of the nuclear recoil direction, due to the alternate sweeping of the WIMP cloud by the rotating Earth. Detection of this effect requires gaseous detectors or anisotropic response scintillators (stilbene). The second is a few percent annual modulation of the recoil rate due to the Earth speed adding to or subtracting from the speed of the Sun. This tiny effect can only be detected with large masses; nuclear recoil identification should also be performed, as the otherwise much larger background may also be subject to seasonal modulation.

The DAMA collaboration has reported results from a total of 6 years exposure with the LIBRA phase involving 250 kg of detectors, plus the earlier 6 years exposure of the original DAMA/NaI experiment with 100 kg of detectors [34], for a cumulated exposure of 1.17 t·y. They observe an annual modulation of the signal in the 2 to 6 keVee bin, with the expected period (1 year) and phase (maximum around June 2), at 8.9 σ level. If interpreted within the standard halo model described above, two possible explanations have been proposed: a WIMP with $m_\chi \simeq 50$ GeV and $\sigma_{\chi p} \simeq 7 \cdot 10^{-6}$ pb (central values)

or at low mass, in the 6 to 10 GeV range with $\sigma_{\chi p} \sim 10^{-3}$ pb; the cross section could be somewhat lower if there is a significant channeling effect [1].

Interpreting these observations as positive WIMP signal raises several issues of internal consistency. First, the proposed WIMP solutions would induce a sizeable fraction of nuclear recoils in the total measured rate in the 2 to 6 keVee bin. No pulse shape analysis has been reported by the authors to check whether the unmodulated signal was detectable this way. Secondly, the residual e/γ-induced background, inferred by subtracting the signal predicted by the WIMP interpretation from the data, has an unexpected shape [35], starting near zero at threshold and quickly rising to reach its maximum near 3 to 3.5 keVee; from general arguments one would expect the background (e.g. due to electronic noise) to increase towards the threshold. Finally, the amplitude of the annual modulation shows a somewhat troublesome tendency to decrease with time. The original DAMA data, taken 1995 to 2001, gave an amplitude of the modulation of 20.0 ± 3.2 in units of 10^{-3} counts/(kg·day·keVee), in the 2-6 keVee bin. During the first phase of DAMA/LIBRA, covering data taken between 2003 and 2007, this amplitude became 10.7 ± 1.9, and in the second phase of DAMA/LIBRA, covering data taken between 2007 and 2009, it further decreased to 8.5 ± 2.2. The ratio of amplitudes inferred from the DAMA/LIBRA phase 2 and original DAMA data is 0.43 ± 0.13, differing from the expected value of 1 by more than 4 standard deviations. (The results for the DAMA/LIBRA phase 2 have been calculated by us using published results for the earlier data alone [36] as well as for the latest grand total [34].) Similar conclusions can be drawn from analyses of the 2-4 and 2-5 keVee bins.

Concerning compatibility with other experiments (see below), the high mass solution is clearly excluded by several null observations (CDMS, EDELWEISS, XENON), while possibly a small parameter space remains available for the low mass solution (according to [35] this possibility is excluded if the energy spectrum measured by DAMA/LIBRA is taken into account). It should be noted that these comparisons have to make assumptions about the WIMP velocity distribution (see above), but varying this within reasonable limits does not resolve the tension [35]. Moreover, one usually assumes that the WIMP scatters elastically, and that the spin-independent cross section for scattering off protons and neutrons is roughly the same. These assumptions are satisfied by all models we know that are either relatively simple (i.e. do not introduce many new particles) or have independent motivation (e.g. attempting to solve the hierarchy problem). As noted earlier, recently models have been constructed where these assumptions do not hold, but at least some of these are no longer able to make the WIMP interpretation of the DAMA(/LIBRA) observations compatible with all null results from other experiments. Finally, appealing to spin-dependent interactions does not help, either [37], in view of null results from direct searches as well as limits on neutrino fluxes from the Sun (see the subsection on indirect WIMP detection below).

No other annual modulation analysis with comparable sensitivity has been reported by any experiment. ANAIS [30], a 100 kg NaI(Tl) project planned to be run at the Canfranc lab, is in the phase of crystal selection and purification. DM-ice is a new project with the aim of checking the DAMA/LIBRA modulation signal in the southern hemisphere. It will consist of 250 kg of NaI(Tl) installed in the heart of the IceCube array. The counting

rate of crystals from the previous NAIAD array recently measured in situ is currently dominated by internal radioactivity.

KIMS [38], an experiment operating 12 crystals of CsI(Tl) with a total mass of 104.4 kg in the Yang Yang laboratory in Korea, has accumulated several years of continuous operation. They should soon be able to set an upper limit on annual modulation amplitude lower than DAMA value if no annual modulation is present, or confirm the DAMA value at 3 σ.

At mK temperature, the simultaneous measurement of the phonon and ionization signals in semiconductor detectors permits event by event discrimination between nuclear and electronic recoils down to 5 to 10 keV recoil energy. This feature is being used by the CDMS [30] and EDELWEISS [30] collaborations. Surface interactions, exhibiting incomplete charge collection, are an important residual background, which is treated by two different techniques: CDMS uses the timing information of the phonon pulse, while EDELWEISS uses the ionization pulses in an interleaved electrodes scheme. New limits on the spin-independent coupling of WIMPs were obtained by CDMS, after operating 19 Germanium cryogenic detectors at the Soudan mine during new runs involving a total exposure of around 612 kg·d (around 300 kg·d fiducial) [39]. Two events were found in the pre-defined signal region, while 0.9 background event were expected. Given these figures, no observation of a signal is claimed. While this data set alone provided a worse limit than the previous runs, the combined data sets provide an improved upper limit on the spin-independent cross section for the scattering of a 70 GeV/c^2 WIMP on a nucleon of 3.8×10^{-8} pb, at 90% CL. The *"WIMP safe"* minimal mass (see the discussion at the end of sec. 1.2.4) of this analysis is about 12 GeV.

An independent analysis of data at low energy (i.e. above 2 keV recoil energy) has also been performed by CDMS [40]. From the knowledge of the quenching factor of Germanium recoils down to 2 keV recoil energy, the energy spectrum is reconstructed using only the measured phonon energy. The obtained spectrum, once corrected for quenching, has a shape somewhat similar to that reported by CoGeNT, but with a lower amplitude (especially for one of the detector modules, which was used to set the limit) so that CDMS concludes that their data are inconsistent with the original WIMP interpretation of the CoGeNT data (note that both detectors use the same target material, so this comparison really is model-independent), as well as with the standard WIMP interpretation of the DAMA data. New detectors with interleaved electrode schemes are being built.

EDELWEISS has operated ten 400 g Germanium detectors equipped with different thermal sensors and an interdigitised charge collection electrode scheme, during one year at the Laboratoire Souterrain de Modane [41]. A total of 5 events were observed in the signal region for a fiducial exposure of 384 kg·d, while 3 events were expected from backgrounds. No WIMP signal was claimed. A similar sensitivity to CDMS is obtained at high mass, while the high 20 keV analysis threshold induces a somewhat poorer limit at masses lower than 50 GeV. New larger detectors with a complete coverage of the crystal with annular electrodes, and better rejection of non-recoil events are being built.

Given their similar sensitivities, the two collaborations combined their data sets. Using a simple combination method, a gain of 1.6 relative to the best limit has been obtained

at WIMP masses larger than 700 GeV, and an improved limit of 3.3×10^{-8} pb for a 90 GeV WIMP mass [42].

The cryogenic experiment CRESST [30] uses the scintillation of $CaWO_4$ as second variable for background discrimination. CRESST has recently submitted for publication [43] the result of the analysis of 730 kg·d exposure performed with 8 detectors. The observation of 67 events in the signal region does not match the about 40 expected background events, originating from e/γ leakage, neutron recoils, as well as leakage from α and Pb recoils. The event excess is said to be compatible with WIMPs. A likelihood method provides two solutions, respectively for 12 and 25 GeV masses, stating also that the background hypothesis alone is more than 4 sigma away from the observed data. However, some other potential sources of background are insufficiently adressed, like "no-light" events, a category of events which previously plagued the sensitivity of this experiment.

Other inorganic scintillators are also being explored, e.g. by the ROSEBUD collaboration [30].

The experimental programs of CDMS II, EDELWEISS II and CRESST II aim at an increase of sensitivity by a factor of 10, by operating around 40 kg of detectors. The next stage SuperCDMS and EURECA-I (a combination of EDELWEISS and CRESST) projects will involve typically 150 kg of detectors. Then GEODM and EURECA-2 will turn to 1 t goals.

Noble gas detectors for dark matter detection are now being developed rapidly by several groups [1]. Dual (liquid and gas) phase detectors allow to measure both the primary scintillation and the ionization electrons drifted through the liquid and amplified in the gas, which is used for background rejection.

The XENON collaboration [30] has successfully operated the 161 kg XENON100 setup at Gran Sasso laboratory during a 100 day data taking period. Within a fiducial mass of 48 kg, 3 events were observed in the signal region, while 1.8 were expected, out of which 1.2 originate from a sizeable contamination of Krypton 85 in the liquid [29]. This allowed to set the best limits at all masses on spin-independent interactions of WIMPs, with a minimum of cross section at 7.0×10^{-9} pb for a mass of 50 GeV. However, the reliability of limits set at masses lower than 10 GeV, especially wrt the relative light efficiency factor, have been discussed in the community. Moreover, as underlined near the end of section 1.2.4, the limits at low mass can be set *only* thanks to the poor energy resolution at threshold –8.4 keV– due to the low photoelectron yield of 0.5 pe/keV. With infinite energy resolution, a Xe detector *with the same threshold of 8.4 keV* is not sensitive to a WIMP mass of 7 GeV. Folding in the XENON100 resolution, the expected fraction of a 7 GeV WIMP signal above 8.4 keV is around 0.05 % (in strong contrast with the 10 % to which CoGeNT is sensitive). If one follows the recommendation made above, the *"WIMP safe"* minimal mass for XENON100 is around 12 GeV.

A reanalysis of part of the XENON10 data [44], using the ionization signal only, with an ionization yield of around 3.5 electron/keV at a threshold of 1.4 keV, sets a more convincing limit in the 7 GeV range, about one order of magnitude below the original CoGeNT claim (see above). The *"WIMP safe"* minimal mass for this XENON10

analysis is around 5 GeV. The XENON10 limit for spin dependent WIMPs with pure neutron couplings is still the best published limit at all masses [45](but likely to be soon superseded by an analysis of XENON100 data). XENON1t, the successor of XENON100 planned to be run at Gran Sasso lab, is in its preparation phase. One should note that, presumably, the planned increase of distance between planes of PMT's will lead to a lower photoelectron yield for scintillation light than at XENON100. This was the case when going from XENON10 (around 1 pe/keV) to XENON100 (around 0.5 pe/keV). For comparison, a 0.25 pe yield per keV would correspond to a *"WIMP safe"* mass of order of 20 GeV.

A new liquid Xenon based project, PANDA-X, with pancake geometry, planned to be housed in the new Jinping lab, will perform a dedicated low mass WIMP search.

ZEPLIN III [30], using a similar principle and with an active mass of 12 kg of Xenon, operated in the Boulby laboratory, has been upgraded for a lower background, has acquired new data, and is now stopped. XMASS [30] in Japan is close to operate a single-phase 800 kg detector (100 kg fiducial mass) installed in a large pure water shield at the SuperKamiokande site. With no pulse shape analysis, the expected performance relies heavily on the self-shielding effect to lower the background [1].

The LUX detector [1], a 300 kg double phase Xenon detector, planned to be operated in the new SURF (previous Sanford) laboratory in US, is in the commissioning phase, in a water shield at surface, before transport underground to the 4850 level.

The WARP collaboration [30] is currently installing a 100 l Argon detector at the Gran Sasso laboratory. Thanks to a double-background rejection method based on the asymmetry between scintillating and ionizing pulses and extremely efficient pulse shape discrimination of scintillating pulses, it looks possible to achieve very high background rejection, even in the presence of the radioactive isotope ^{39}Ar. The ArDM project [30] is using a similar technique with a much larger (1,100 kg) mass. It should be installed soon and take data at the newly opened Canfranc laboratory. MiniCLEAN and DEAP-3600 [30], both measuring only scintillation signals in spherical geometries in single phase mode, are being assembled at SNOLab and will operate respectively 500 kg of Ar/Ne and 3600 kg of Ar [1]. DARK SIDE [30], is another Argon based, double phase project, involving in a first step about 50 kg of ^{39}Ar depleted Argon, to be installed in Gran Sasso lab.

The low pressure Time Projection Chamber technique is the only convincing way to measure the direction of nuclear recoils and prove the galactic origin of a possible signal [1]. The DRIFT collaboration [30] has operated a 1 m^3 volume detector in the UK Boulby mine. Though the background due to internal radon contamination was lowered, no new competitive limit has yet been set. The MIMAC collaboration [30] is investigating a sub-keV energy threshold TPC detector. Additional sensitive measurements of Fluor nuclei quenching factor and recoil imaging have been performed recently by this group down to few keV. A 2.5 l 1000 channel prototype is going to be operated soon in the Fréjus laboratory. Other groups developing similar techniques, though with lower sensitivity, are DMTPC in the US and NewAge in Japan.

The following more unconventional detectors use ^{19}F nuclei to set limits on the spin

dependent coupling of WIMPs, with less than kg mass detectors. The bubble chamber like detector, COUPP [30], run at Fermilab, has provided a new limit [46] for spin dependent proton coupling WIMPs for masses above 20 GeV, superseding an earlier KIMS result. PICASSO [30], a superheated droplet detector run at SNOLAB, obtained a better limit below 20 GeV on the same type of WIMPs [47]. Finally, SIMPLE [30], a similar experiment run at Laboratoire Souterrain de Rustrel, submitted results for publication that claim to provide the currently best limit on the spin-dependent WIMP-proton cross section for all WIMP masses [48].

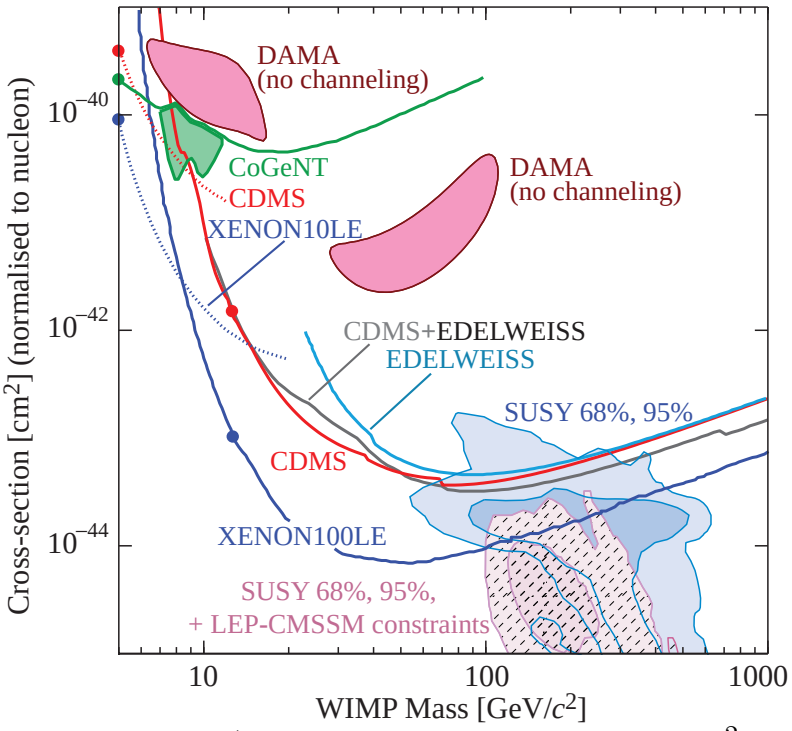

Figure 22.1: Cross sections (normalised to nucleon assuming A^2 dependence, see section 1.2.4) for spin independent coupling versus mass diagrams. References to the experimental results are given in the text. The big dots on some curves show the *"WIMP safe"* minimal mass for the corresponding experimental result (see details in text). DAMA candidates region (no channeling) are from [50], shaded 68% and 95% regions are SUSY predictions by [51], together with recent constraints (crosshatched 68% and 95% regions) set by LHC experiments (CMSSM) [52]. Here equal cross sections for scattering from protons and neutrons have been assumed.

Figures 22.1 and 22.2 illustrate the limits and positive claims forf cross sections, normalised to nucleon, for spin independent and spin dependent couplings, respectively, as functions of WIMP mass, where only the two currently best limits are presented. Also shown are constraints from indirect observations (see the next section) and typical regions of SUSY models, before and after recent LHC results. These figures have been made with the `dmtools` web page, thanks to the very efficient collaboration of dmtools team [55].

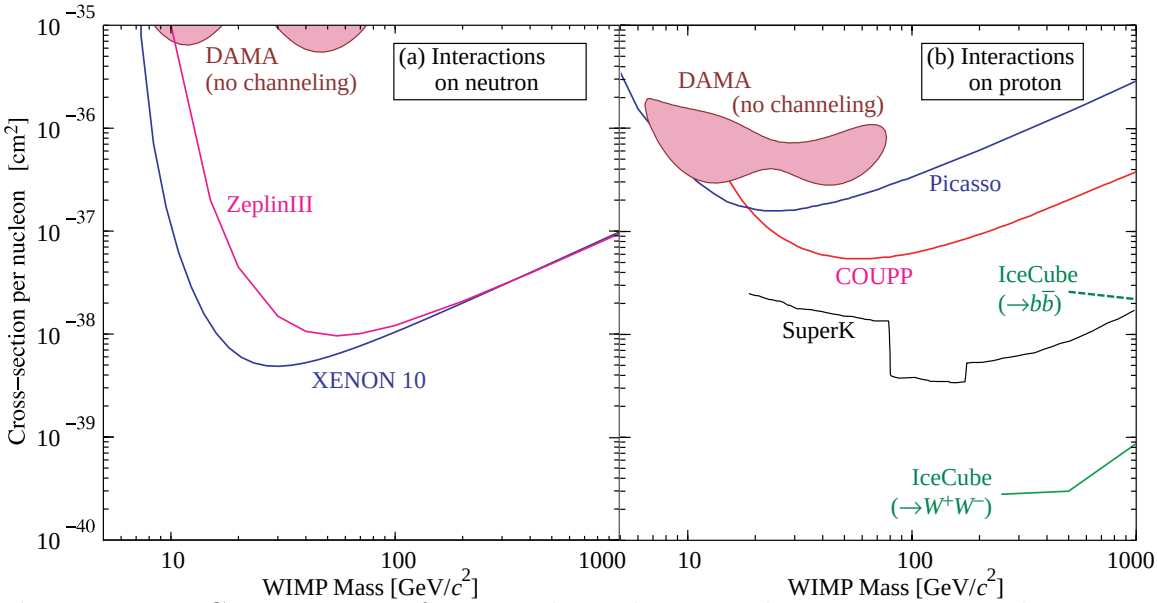

Figure 22.2: Cross sections for spin dependent coupling versus mass diagrams. References to the experimental results are given in the text. The DAMA candidates region (no channeling) are from [50]: (a) interactions on neutron; (b) interactions on proton.

Sensitivities down to $\sigma_{\chi p}$ of 10^{-10} pb, as needed to probe large regions of MSSM parameter space [27], will be reached with detectors of typical masses of 1 ton, assuming nearly perfect background discrimination capabilities. Note that the expected WIMP rate is then 5 evts/ton/year for Ge. The ultimate neutron background will only be identified by its multiple interactions in a finely segmented or multiple-interaction-sensitive detector, and/or by operating detectors containing different target materials within the same set-up. Larger mass projects are envisaged by the DARWIN European consortium and the MAX project in the US (liquid Xe and Ar multiton project) [30].

22.2.6. *Status and prospects of indirect WIMP searches* :

WIMPs can annihilate and their annihilation products can be detected; these include neutrinos, gamma rays, positrons, antiprotons, and antinuclei [1]. These methods are complementary to direct detection and might be able to explore higher masses and different coupling scenarios. "Smoking gun" signals for indirect detection are GeV neutrinos coming from the center of the Sun or Earth, and monoenergetic photons from WIMP annihilation in space.

WIMPs can be slowed down, captured, and trapped in celestial objects like the Earth or the Sun, thus enhancing their density and their probability of annihilation. This is a source of muon neutrinos which can interact in the Earth. Upward going muons can then be detected in large neutrino telescopes such as MACRO, BAKSAN, SuperKamiokande, Baikal, AMANDA, ANTARES, NESTOR, and the large sensitive area IceCube [1]. The best upper limit for relatively soft muons, of $\simeq$ 1000 muons/km^2/year for muons with energy above $\sim$ 2 GeV [53], comes from SuperKamiokande [30] using through-going

muons. For more energetic muons a slightly more stringent limit has been set by IceCube22 (using 22 strings), e.g. excluding a flux above 610 muons/km^2/year from the Sun for a WIMP model with average muon energy of 150 GeV [54]. In the framework of the MSSM and with standard halo velocity profiles, only the limits from the Sun, which mostly probe spin-dependent couplings, are competitive with direct WIMP search limits. IceCube80 [30] will increase this sensitivity by a factor $\simeq 5$ at masses higher than 200 GeV while IceCube Deep Core will allow to reach masses down to 50 GeV [1].

WIMP annihilation in the halo can give a continuous spectrum of gamma rays and (at one-loop level) also monoenergetic photon contributions from the $\gamma\gamma$ and γZ channels. These channels also allow to search for WIMPs for which direct detection experiments have little sensitivity, *e.g.*, almost pure higgsinos. However, the size of this signal depends very strongly on the halo model, but is expected to be most prominent near the galactic center. The central region of our galaxy hosts a strong TeV point source discovered [56] by the H.E.S.S. Cherenkov telescope [57]. Moreover, FERMI/LAT [30] data revealed a new extended source of GeV photons near the galactic center above and below the galactic plane [58]. Both of these sources are most likely of astrophysical origin. The presence of these unexpected backgrounds makes it more difficult to discover WIMPs in this channel, and no convincing signal has been claimed. FERMI/LAT observations of the galactic halo are in agreement with predictions based on purely astrophysical sources (in contrast to a re-analysis of earlier EGRET data [59]) , and rule out many WIMP models that were constructed to explain the PAMELA and FERMI/LAT excesses in the $e^{\pm}$ channel [60]. Similarly, Cherenkov telescope and FERMI/LAT observations of nearby dwarf galaxies, globular clusters, and clusters of galaxies only yielded upper limits on photon fluxes from WIMP annihilation. While limits from individual observations are still above the predictions of most WIMP models, a very recent combination [61] of limits from dwarf galaxies excludes WIMPs annihilating hadronically with the standard cross section needed for thermal relics, if the WIMP mass is below 25 GeV; assumptions are annihilation from an $S-$wave initial state, and a dark matter density distribution scaling like the inverse of the distance from the center of the dwarf galaxy at small radii.

Antiparticles arise as additional WIMP annihilation products in the halo. To date the best measurement of the antiproton flux comes from the PAMELA satellite [30], and covers kinetic energies between 60 MeV and 180 GeV [62]. The result is in good agreement with secondary production and propagation models. These data exclude WIMP models that attempt to explain the $e^{\pm}$ excesses via annihilation into $W^{\pm}$ or Z^0 boson pairs; however, largely due to systematic uncertainties they do not significantly constrain conventional WIMP models.

The best measurements of the positron (and electron) flux at (tens of) GeV energies again comes from PAMELA [63], showing a rather marked rise of the positron fraction between 10 and 100 GeV. The observed spectrum falls within the one order of magnitude span (largely due to differences in the propagation model used) of positron fraction values predicted by secondary production models [64]. Measurements of the total electron+positrons energy spectrum by ATIC [65], FERMI/LAT [66] and H.E.S.S. [67] between 100 and 1000 GeV also exceed the predicted purely secondary spectrum, but with very large dispersion of the magnitude of these excesses. While it has been recognized

that astrophysical sources may account for all these features, many ad-hoc Dark Matter models have been built to account for these excesses. As mentioned in section 1, given the amount of jerking and twisting needed to build such models not to contradict any observation, it seems very unlikely that Dark Matter is at the origin of these excesses.

Last but not least, an antideuteron signal [1], as potentially observable by AMS2 or PAMELA, could constitute a signal for WIMP annihilation in the halo.

An interesting comparison of respective sensitivities to MSSM parameter space of future direct and various indirect searches has been performed with the DARKSUSY tool [68]. A web-based up-to-date collection of results from direct WIMP searches, theoretical predictions, and sensitivities of future experiments can be found in [55]. Also, the web page [69] allows to make predictions for WIMP signals in various experiments, within a variety of SUSY models and to extract limits from simply parametrised data. Integrated analysis of all data from direct and indirect WIMP detection, and also from LHC experiments should converge to a comprehensive approach, required to fully unravel the mysteries of dark matter.

References:

1. For details, recent reviews and many more references about particle dark matter, see G. Bertone, *Particle Dark Matter* (Cambridge University Press, 2010).
2. For a brief but delightful history of DM, see V. Trimble, in *Proceedings of the First International Symposium on Sources of Dark Matter in the Universe*, Bel Air, California, 1994, published by World Scientific, Singapore (ed. D.B. Cline). See also the recent review G. Bertone, D. Hooper, and J. Silk, Phys. Rep. **405**, 279 (2005).
3. See *Cosmological Parameters* in this *Review*.
4. B. Paczynski, Astrophys. J. **304**, 1 (1986);
   K. Griest, Astrophys. J. **366**, 412 (1991).
5. F. De Paolis *et al.*, Phys. Rev. Lett. **74**, 14 (1995).
6. R. Catena and P. Ullio, JCAP **1008**, 004 (2010).
7. M. Pato *et al.*, Phys. Rev. **D82**, 023531 (2010).
8. K. Kohri, D.H. Lyth, and A. Melchiorri, JCAP **0804**, 038 (2008).
9. See *Axions and Other Very Light Bosons* in this *Review*.
10. A. Kusenko, Phys. Reports **481**, 1 (2009).
11. E.W. Kolb and M.E. Turner, *The Early Universe*, Addison-Wesley (1990).
12. For a general introduction to SUSY, see the section devoted in this *Review of Particle Physics*. For a review of SUSY Dark Matter, see G. Jungman, M. Kamionkowski, and K. Griest, Phys. Reports **267**, 195 (1996).
13. See *Searches for WIMPs and Other Particles* in this *Review*.
14. S. Dimopoulos, G.F. Giudice, and A. Pomarol, Phys. Lett. **B389**, 37 (1996).
15. M. Cirelli and J.M. Cline, Phys. Rev. **D82**, 023503 (2010).
16. T. Moroi and L. Randall, Nucl. Phys. **B570**, 455 (2000).
17. R. Allahverdi and M. Drees, Phys. Rev. Lett. **89**, 091302 (2002).
18. M. Fujii and T. Yanagida, Phys. Lett. **B542**, 80 (2002).
19. J. Hisano, K. Kohri, and M.M. Nojiri, Phys. Lett. **B505**, 169 (2001).
20. D.E. Kaplan, M.A. Luty, and K.M. Zurek, Phys. Rev. **D79**, 115016 (2009).

21. MACHO Collab., C. Alcock *et al.*, Astrophys. J. **542**, 257 (2000);
EROS Collab., AA **469**, 387 (2007);
OGLE Collab., arXiv:1106.2925 [astro-ph.GA],(MNRAS, to appear).
22. http://www.phys.washington.edu/groups/admx/home.html.
23. S.J. Asztalos *et al.*, Phys. Rev. **D69**, 011101 (2004);
S.J. Asztalos *et al.*, Phys. Rev. Lett. **104**, 041301 (2010).
24. L.D. Duffy *et al.*, Phys. Rev. **D74**, 012006 (2006).
25. M. Shibata *et al.*, J. Low Temp. Phys. **151**, 1043 (2008);
M. Tada *et al.*, Phys. Lett. **A349**, 488 (2006).
26. M.C. Smith *et al.*, Mon. Not. R. Astron. Soc. **379**, 755 (2007).
27. J. Ellis *et al.*, Phys. Rev. **D77**, 065026 (2008).
28. C.E. Aalseth *et al.*, Phys. Rev. Lett. **106**, 131301 (2011).
29. XENON100 Collab., E. Aprile *et al.*, arXiv:1104.2549, sumbmitted to PRL.
30. A very useful collection of web links to the homepages of Dark Matter related conferfences, and of experiments searching for WIMP Dark Matter, is the "Dark Matter Portal" at http://lpsc.in2p3.fr/mayet/dm.php.
31. http://cogent.pnnl.gov/.
32. C.E. Aalseth *et al.*, Phys. Rev. Lett. **107**, 141301 (2011).
33. P.J. Fox *et al.*, arXiv:1107.0717v2;
T. Schwetz and J. Zupan, JCAP **1108**, 008 (2011).
34. DAMA Collab., R. Bernabei *et al.*, Eur. Phys. J. **C67**, 39 (2010).
35. M. Fairbairn and T. Schwetz, JCAP **0901**, 037 (2009).
36. DAMA Collab., R. Bernabei *et al.*, Eur. Phys. J. **C56**, 333 (2008).
37. C.J. Copi and L.M. Krauss, New Astron. Rev. **49**, 185 (2005).
38. http://q2c.snu.ac.kr/KIMS/KIMS_index.htm.
39. CDMS Collab., Z. Ahmed *et al.*, Science **327**, 1619 (2010).
40. CDMS Collab., Z. Ahmed *et al.*, Phys. Rev. Lett. **06**, 131302 (2011).
41. EDELWEISS Collab., E. Armengaud *et al.*, Phys. Lett. **B702**, 329 (2011).
42. EDELWEISS and CDMS Collab., Z. Ahmed *et al.*, Phys. Rev. **84**, 011102 (2011).
43. CRESST Collab., G. Angloher *et al.*, arXiv:1109.0702 [astro-ph.CO].
44. XENON10 Collab., J Angle *et al.*, Phys. Rev. Lett. **107**, 051301 (2011).
45. XENON10 Collab., J Angle *et al.*, Phys. Rev. Lett. **101**, 091301 (2008).
46. E. Behnke *et al.*, Phys. Rev. Lett. **106**, 021303 (2011).
47. S. Archambault *et al.*, Phys. Lett. **B682**, 185 (2009).
48. M. Felizardo *et al..*, arXiv:1106.3014 [astro-ph.CO].
49. ZEPLIN Collab., V. N. Lebedenko *et al..*, Phys. Rev. Lett. **103**, 151302 (2009).
50. C. Savage *et al..*, JCAP **0904**, 010, 2009.
51. R. Trotta *et al..*, JHEP **0812** 024, 2008.
52. O. Buchmueller *et al..*, Eur. Phys. J. **C71**, 1634 (2011).
53. SuperKamiokande Collab., S. Desai *et al.*, Phys. Rev. **D70**, 083523 (2004).
54. IceCube Collab., R. Abbasi *et al.*, Phys. Rev. Lett. **102**, 201302 (2009).
55. http://dmtools.brown.edu; http://dmtools.brown.edu:8080/.
56. H.E.S.S. Collab., F. Aharonian *et al.*, Astron. Astrophys. **503**, 817 (2009);
H.E.S.S. Collab., F. Acero *et al.*, MNRAS **402**, 1877 (2010).

57. http://www.mpi-hd.mpg.de/hfm/HESS/.
58. M. Su, T.R. Slatyer, and D.P. Finkbeiner, Astrophys. J. **724**, 1044 (2010).
59. W. de Boer *et al.*, Astron. Astrophys. **444**, 51 (2005), and Phys. Lett. **B636**, 13 (2006).
60. A.A. Abdo *et al.*, JCAP **1004**, 014 (2010).
61. Fermi-LAT Collab., M. Ackermann et al., arXiv:1108.3546 [astro-ph].
62. PAMELA Collab, O. Adriani *et al.*, Phys. Rev. Lett. **105**, 121101 (2010).
63. PAMELA collab, O. Adriani *et al.*, Nature **458**, 607 (2009).
64. T. Delahaye *et al.*, Astronomy and Astrophysics **501**, 821 (2009).
65. ATIC collab, J. Chang *et al.*, Nature (London) **456**, 362 (2008).
66. FERMI/LAT collab, A.A. Abdo *et al.*, Phys. Rev. Lett. **102**, 181101 (2009).
67. HESS collab, F. Aharonian *et al.*, Phys. Rev. Lett. **101**, 261104 (2008).
68. DARKSUSY site: http://www.physto.se/ edsjo/darksusy/.
69. ILIAS web page: http://pisrv0.pit.physik.uni-tuebingen.de/darkmatter/.